


# Proton irradiation-induced dynamic characteristics on high performance GaN/AlGaN/GaN Schottky barrier diodes

Tao Zhang(张涛), Ruo-Han Li(李若晗), Kai Su(苏凯), Hua-Ke Su(苏华科), Yue-Guang Lv(吕跃广), Sheng-Rui Xu(许晟瑞), Jin-Cheng Zhang(张进成), and Yue Hao(郝跃)

**Citation:**Chin. Phys. B, 2023, 32 (**8**): 087301. DOI: 10.1088/1674-1056/acbded

Journal homepage: http://cpb.iphy.ac.cn; http://iopscience.iop.org/cpb

**What follows is a list of articles you may be interested in**

---

## Proton irradiation-induced dynamic characteristics on high performance GaN/AlGaN/GaN Schottky barrier diodes

Tao Zhang(张涛), Ruo-Han Li(李若晗), Kai Su(苏凯), Hua-Ke Su(苏华科), Yue-Guang Lv(吕跃广), Sheng-Rui Xu(许晟瑞), Jin-Cheng Zhang(张进成), and Yue Hao(郝跃)

Chin. Phys. B, 2023, 32 (**8**): 087301. DOI: 10.1088/1674-1056/acbded

## Low-resistance ohmic contacts on InAlN/GaN heterostructures with MOCVD-regrown $n^+$-InGaN and mask-free regrowth process

Jingshu Guo(郭静姝), Jiejie Zhu(祝杰杰), Siyu Liu(刘思雨), Jielong Liu(刘捷龙), Jiahao Xu(徐佳豪), Weiwei Chen(陈伟伟), Yuwei Zhou(周雨威), Xu Zhao(赵旭), Minhan Mi(宓珉瀚), Mei Yang(杨眉), Xiaohua Ma(马晓华), and Yue Hao(郝跃)

Chin. Phys. B, 2023, 32 (**3**): 037303. DOI: 10.1088/1674-1056/ac891b

## Design optimization of high breakdown voltage vertical GaN junction barrier Schottky diode with high-*K*/low-*K* compound dielectric structure

Kuiyuan Tian(田魁元), Yong Liu(刘勇), Jiangfeng Du(杜江锋), and Qi Yu(于奇)

Chin. Phys. B, 2023, 32 (**1**): 017306. DOI: 10.1088/1674-1056/ac8e99

## Protection of isolated and active regions in AlGaN/GaN HEMTs using selective laser annealing

Mingchen Hou(侯明辰), Gang Xie(谢刚), Qing Guo(郭清), and Kuang Sheng(盛况)

Chin. Phys. B, 2021, 30 (**9**): 097302. DOI: 10.1088/1674-1056/abf34c

## Analysis of the decrease of two-dimensional electron gas concentration in GaN-based HEMT caused by proton irradiation

Jin-Jin Tang(汤金金), Gui-Peng Liu(刘贵鹏), Jia-Yu Song(宋家毓), Gui-Juan Zhao(赵桂娟), and Jian-Hong Yang(杨建红)

Chin. Phys. B, 2021, 30 (**2**): 027303. DOI: 10.1088/1674-1056/abbbf7

---

# Proton irradiation-induced dynamic characteristics on high performance GaN/AlGaN/GaN Schottky barrier diodes

Tao Zhang(张涛)[1], Ruo-Han Li(李若晗)[2], Kai Su(苏凯)[1], Hua-Ke Su(苏华科)[1], Yue-Guang Lv(吕跃广)[3], Sheng-Rui Xu(许晟瑞)[1,†], Jin-Cheng Zhang(张进成)[1,‡], and Yue Hao(郝跃)[1]

[1] *Key Laboratory of Wide Band-Gap Semiconductors and Devices, School of Microelectronics, Xidian University, Xi'an* 710071, *China*
[2] *Xi'an Microelectronics Technology Institute, Xi'an* 710054, *China*
[3] *School of Aerospace Science and Technology, Xidian University, Xi'an* 710071, *China*

(Received 14 October 2022; revised manuscript received 20 February 2023; accepted manuscript online 22 February 2023)

Dynamic characteristics of the single-crystal GaN-passivated lateral AlGaN/GaN Schottky barrier diodes (SBDs) treated with proton irradiation are investigated. Radiation-induced changes including idealized Schottky interface and slightly degraded on-resistance ($R_{ON}$) are observed under 10-MeV proton irradiation at a fluence of $10^{14}$ cm$^{-2}$. Because of the existing negative polarization charges induced at GaN/AlGaN interface, the dynamic ON-resistance ($R_{ON,dyn}$) shows negligible degradation after a 1000-s-long forward current stress of 50 mA to devices with and without being irradiated by protons. Furthermore, the normalized $R_{ON,dyn}$ increases by only 14% that of the initial case after a 100-s-long bias of −600 V has been applied to the irradiated devices. The high-performance lateral AlGaN/GaN SBDs with tungsten as anode metal and *in-situ* single-crystal GaN as passivation layer show a great potential application in the harsh radiation environment of space.

**Keywords:** AlGaN/GaN SBDs, GaN passivation layer, proton irradiation, dynamic on-resistance

**PACS:** 73.40.Kp, 85.30.De, 85.30.Kk **DOI:** 10.1088/1674-1056/acbded

## 1. Introduction

Because of the great properties of the AlGaN/GaN heterostructure with high density and high mobility two dimensional electron gas (2DEG), and high critical field, the AlGaN/GaN devices have been proven to be promising a candidate in the next-generation power-switching applications.[1–5] As for the hexagonal GaN, the lattice constant $a$ and $c$ are 0.319 nm and 0.519 nm, respectively, which are smaller than the counterparts for the traditional narrow bandgap semiconductor Si and GaAs. Small lattice constant or wide bandgap of semiconductor always corresponds to high displacement threshold energy and an impressive radiation hardness property.[6,7] The high radiation tolerance of GaN-based device makes it suitable for deployment aboard space-based systems.[8–10] Meanwhile, the compatible fabrication process between AlGaN/GaN Schottky barrier diodes (SBDs) and high electron mobility transistors (HEMTs) shows a great promise for monolithic integration with improved characteristics and suppressed chip volume, which is vital for the space vehicles.[11–13]

In order to improve the rectification efficiency, SBDs with low turn-on voltage ($V_{ON}$), low reverse leakage current ($I_R$), and high breakdown voltage (BV) are essential. The AlGaN/GaN SBDs with fully recessed anode structure are conducive to suppressing $I_R$ by avoiding the effect of threading dislocation formed in the epitaxial process, and the direct contact between low work-function anode metal and nonpolar face of GaN channel is able to reduce the $V_{ON}$ and improve the forward current density.[14–16] Recently, the AlGaN/GaN devices with a thick *in-situ* GaN cap layer as a passivation layer was proposed to reduce the influence of surface states, showing the impressive stability of the dynamic ON-resistance ($R_{ON,dyn}$) under long-duration stress.[17–19]

In this work, the *in-situ* single-crystal GaN-passivated AlGaN/GaN SBDs with fully recessed anode structure and low work-function metal as anode are irradiated by 10-MeV protons at a fluence of $10^{14}$ cm$^{-2}$. The interface characteristics and dynamic performances of the fabricated AlGaN/GaN SBDs irradiated by proton are preliminary studied. The irradiation treatment idealizes the metal/semiconductor (M/S) interface, and the Schottky interface parameter such as the ideality factor ($\eta$) changed towards the ideal case. Furthermore, $R_{ON,dyn}$, which is sensitive to the traps existing in the surface, the passivation layer, the barrier layer and the GaN bulk, becomes only 1.14 times the static $R_{ON}$ after being acted on by a 100-s-long bias of −600 V, and 1.04 times after being experienced by a 1000-s-long bias of 50 mA, for the irradiated AlGaN/GaN SBDs.

## 2. Device fabrication

The epitaxial layers were grown via metal–organic chemical-vapor deposition (MOCVD) on a sapphire sub-

†Corresponding author. E-mail: srxu@xidian.edu.cn
‡Corresponding author. E-mail: jchzhang@xidian.edu.cn

© 2023 Chinese Physical Society and IOP Publishing Ltd 

strate, which consist of an 80-nm GaN cap layer, a 25-nm $Al_{0.25}Ga_{0.75}N$ barrier layer, a 1-nm AlN space layer, a 200-nm GaN channel layer, a 2.4-μm undoped GaN buffer layer, and a 45-nm AlN nucleation layer, as shown in Fig. 1. The thick single-crystal GaN cap layer acted as the *in-situ* passivation layer, which is not heteroepitaxially grown by plasma-enhanced chemical vapor deposition (PECVD) or low-pressure chemical vapor deposition (LPCVD). The high-quality passivation layer with low density of interface states contributed to the low dispersion under high-voltage stress and thus improved the power output with less $R_{ON,dyn}$ degradation. The undoped GaN buffer layer and the thick GaN cap layer were able to suppress the current collapse under high bias voltage induced by bulk traps and surface traps, respectively.[20–23]

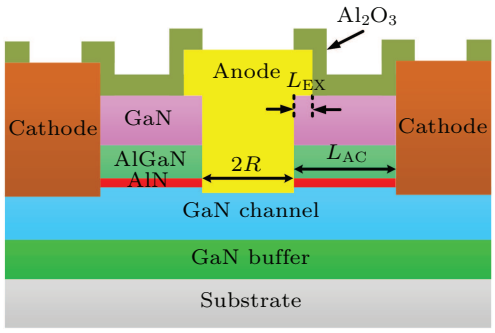



**Fig. 1.** Cross-sectional schematic view of fabricated GaN/AlGaN/GaN SBDs exposed to proton irradiation.

The device fabrication started with device isolation via the inductively coupled plasma (ICP) etching process. The Ohmic metal stacks of Ti/Al/Ni/Au (22/140/55/45 nm) were evaporated after removing the GaN cap layer and AlGaN barrier layer by ICP process, then the electrodes were annealed at 870 °C for 35 s in $N_2$ atmosphere. The recessed anode region was defined via the optimized ICP process with an etch rate of 36 nm/min, followed with the low temperature annealing process to repair the etching damage. Then, the metal stacks of W/Au were sputtered as anode and treated with post anode annealing (PAA) process at 450 °C for 300 s in $N_2$ atmosphere. As for the high-performance GaN SBD fabrication, PAA process was essential to eliminate the interface states at the M/S interface and improve the device performance by suppressing leakage current, increasing forward current density, improving BV, and enhancing devices stability. After that, a 20-nm $Al_2O_3$ was deposited via atomic layer deposition (ALD). Finally, the devices were irradiated with 10-MeV proton at room temperature at fluences of $10^{14}$ $cm^{-2}$.

The fabricated AlGaN/GaN SBDs with a thick GaN cap layer possessed an anode radius ($R$) of 100 μm, an anode-cathode spacing ($L_{AC}$) of 15 μm, and a length ($L_{EX}$) extending over the recessed region of 2 μm. The forward DC and temperature-dependent characteristics were measured with a Keithley 4200 Semiconductor parameter analyzer, and the reverse breakdown and dynamic characteristics were performed by using an Agilent B1505A high-voltage semiconductor analyser system.

## 3. Results and discussion

Figure 2(a) shows the well-behaved forward $I$–$V$ characteristics of the fabricated GaN/AlGaN/GaN SBDs before and after being irradiated by protons. In Fig. 2 and the following, PI stands for proton irradiation. The $V_{ON}$ is defined as the value at an anode current density of 1 mA/mm, and it is 0.38 V for both samples, and the low $V_{ON}$ is benefited from the direct contact between low work-function anode metal and the non-polar sidewall of GaN channel, which shows a great improvement in the static power consumption. The $R_{ON}$ is defined as the value at an anode current density of 100 mA/mm, and it, under the influence of $V_{ON}$, is calculated to be 15.0 Ω·mm and 13.7 Ω·mm for the device with and without irradiated by protons, respectively. The slight degradation of $R_{ON}$ is caused by either a decrease in 2DEG density and saturated carrier velocity induced by the photon radiation.[24,25] The reverse $I$–$V$ characteristics of the fabricated lateral GaN SBD with and without irradiated by protons are shown in Fig. 2(b). Three lateral AlGaN/GaN SBDs are performed on both samples, and all of them show a similar tendency. The reverse $I$–$V$ characteristic of the irradiated sample is different from the counterpart, which is caused by the degradation of GaN material property. Figure 2(c) shows the micro-Raman of the GaN epitaxies before and after being irradiated by protons, and the measured peak position of $E_2^{High}$ and $A_1$ (LO) are 571 $cm^{-1}$ and 735 $cm^{-1}$, respectively, for both samples, indicating that the stress state of the thick GaN cap layer is not affect by proton irradiation. However, the full width at half maximum (FWHM) of $E_2^{High}$ of the irradiated sample increases compared to that of the control sample, which means that the crystal quality of GaN was deteriorated after proton irradiation treatment, and the deteriorated GaN crystal quality resulted in the degenerated reverse $I$–$V$ characteristics.

Figures 3(a) and 3(b) show the temperature-dependent $I$–$V$ characteristics of the fabricated GaN/AlGaN/GaN SBDs before and after being irradiated by protons. The $V_{ON}$ of the irradiated SBD changes from 0.38 V to 0.31 V, while the other one varies from 0.38 V to 0.33 V, and the leakage current increases by 11.87 times for irradiated device, and 22.65 times for the unirradiated device, as the temperature increases from 300 K to 425 K. For the irradiated device, the increase of suppressed leakage current with temperature rising is attributed to the fact that the ideal M/S interface has been treated by the proton irradiation.

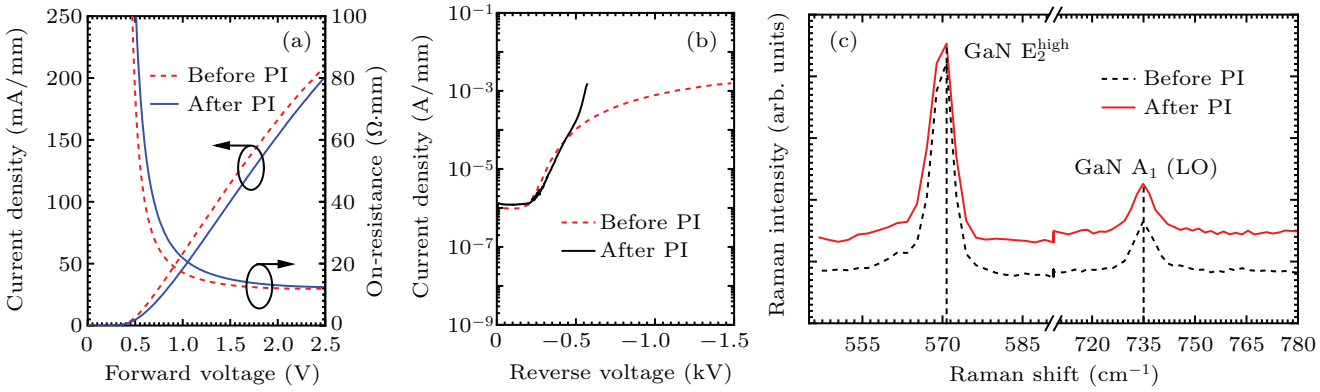



**Fig. 2.** Room-temperature (a) forward *I*–*V* characteristics and extracted $R_{ON}$, (b) reverse *I*–*V* characteristics of fabricated lateral AlGaN/GaN SBD before and after being irradiated by protons. (c) Micro-Raman of GaN epitaxies irradiated by protons.

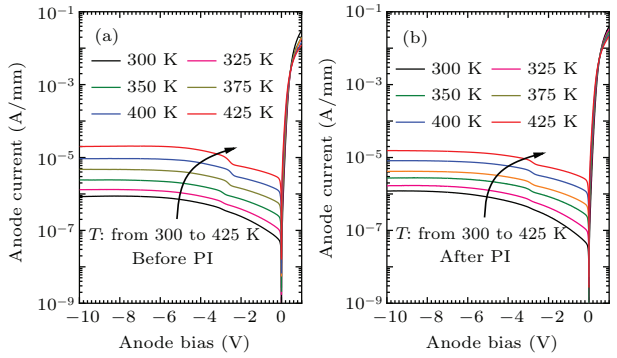



**Fig. 3.** Temperature-dependent *I*–*V* characteristics of fabricated GaN SBD (a) before and (b) after being irradiated by protons.

According to the theory of thermionic emission, the forward *I*–*V* relationship of GaN SBD can be expressed as $I = I_S[\exp(q \times (V - I \times R_S)/(\eta kT) - 1)]$, where $I_S$ is the reverse saturation current which can be determined from the intercept of the $\ln(I)$–$V$ curve, $q$ is the electric charge, $R_S$ is the series resistance, $\eta$ is the ideality factor, $k$ is the Boltzmann constant, and $T$ is the absolute temperature. The extracted Schottky barrier height and ideality factor of the fabricated device before and after being irradiated by protons are shown in Figs. 4(a) and 4(b), respectively. The Schottky barrier height of the irradiated sample increases from 0.56 eV to 0.73 eV, while that of the other sample increases from 0.53 eV to 0.63 eV as the temperature increases from 300 K to 425 K. Ideally, the current transport mechanism of the Schottky junction is based on the theory of thermionic emission, and the ideality factor is equal to unity. The ideality factor of the irradiated SBD is closer to unity than that of the fabricated devices without irradiation treatment, which means that the thermionic emission is dominated in the transport mechanism in a barrier-limited range from 300 K to 425 K. The Schottky barrier height can be expressed as $\Phi_{Bn} = \Phi_M - \chi_S - eV_i$, where $\Phi_M$ is the work-function of anode metal, $\chi_S$ is the affinity energy, and $V_i$ is the interface potential and $V_i$ is contributed by the net charges on the GaN surface, which are induced by the dangling bonds or native oxide layer, and their image charges on the side of anode metal, thereby degenerating the ideal performance of Schottky junction. After proton irradiation treatment, the net charges at Schottky interface are neutralized, with $V_i$ decreasing, which leads the Schottky barrier height increase. Meanwhile, the suppressed interface traps promote the idealized interface property. The increased Schottky barrier height and the reduced ideality factor of the proton-irradiated device show that some reactions occur at the M/S interface in the proton irradiation process and the interface between W anode metal and the recessed GaN surface becomes more ideal.

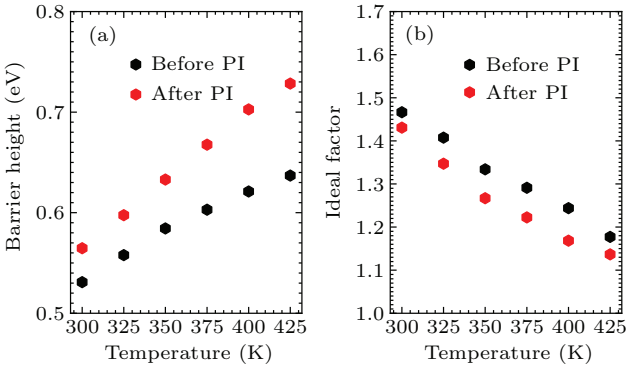



**Fig. 4.** Temperature-dependent (a) Schottky barrier height and (b) ideality factor of fabricated GaN/AlGaN/GaN SBDs before and after being irradiated by protons.

The dynamic performance is more sensitive to the irradiation than DC performance, and the pulse measurements of the fabricated GaN/AlGaN/GaN SBDs with and without being irradiated by protons are carried out by using an Agilent B1505A high-voltage semiconductor analyser system as shown in Fig. 5. The pulse width and period are set to be 5 ms and 100 ms, respectively. Owing to the reduction of interface state after PAA treatment, the enhancement of M/S interface performance, and the thick *in-situ* single-crystal GaN cap layer as the passivation layer, the pulse *I*–*V* characteristics of the fabricated devices show good performance even in the irradiated sample. Figure 5(c) displays the normalized $R_{ON,dyn}$ *versus* anode quiescent base. Because the enhancement of electrons in the active region, the $R_{ON,dyn}$ increases with the static anode quiescent base rising. The $R_{ON.dyn}$ degrades only 35% and 62% at a quiescent base of −100 V compared to a quiescent of 0 V, for devices before and after being irradiated by protons, respectively.

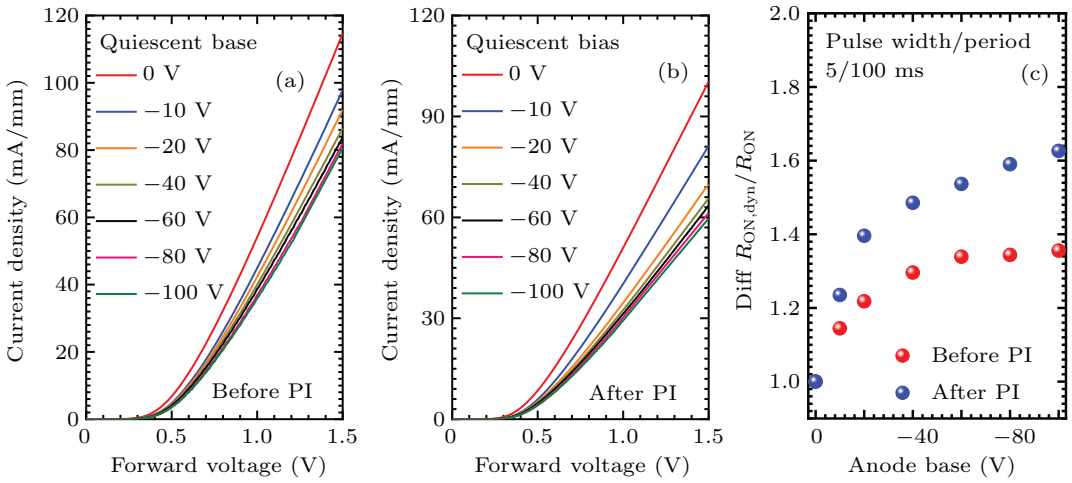



**Fig. 5.** Pulse measurements for fabricated GaN SBDs (a) before and (b) after being irradiated by protons. (c) Extracted differential $R_{ON,dyn}$ *versus* anode quiescent base.

The long-time stress reliability of GaN/AlGaN/GaN SBDs before and after being irradiated by protons are evaluated with a consecutive current stress of 50 mA for 1000 s, and the results are shown in Figs. 6(a) and 6(b), respectively. The anode is based with a steady current of 50 mA with cathode grounded for various stress duration, and then the anode voltage is swept from 0 V to 1.5 V. It is obvious that the forward *I*–*V* characteristics show negligible degradation even under the action of such a long-time stress of 1000 s for both devices. The fabricated lateral GaN SBDs show good performances under the applied long-time forward current stress even for the irradiated devices.

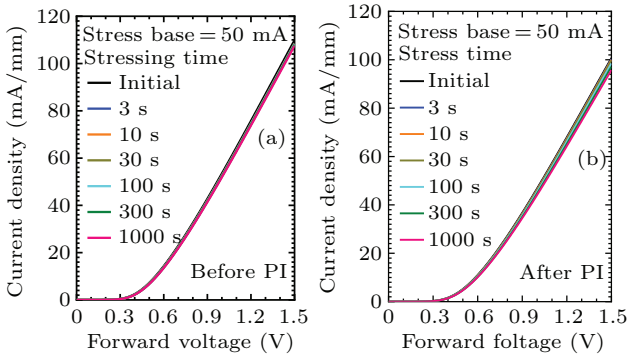



**Fig. 6.** Linear-scale forward *I*–*V* characteristics of fabricated GaN SBDs (a) before and (b) after being irradiated by protons with stress current of 50 mA.

Furthermore, the long-time high-voltage reverse stress reliability is a key parameter when the devices are used as high-voltage power switching. Figures 7(a) and 7(b) exhibit the dynamic performances of the fabricated devices which are evaluated under a consecutive high-voltage stress of −600 V for 100 s before and after proton irradiation, respectively. The high reverse stress voltage of −600 V is applied to the anode electrode, with cathode grounded firstly. After that, the forward anode voltage is swept from 0 V to 1.5 V. The $R_{ON,dyn}$ of the irradiated device only decrease by 14% that of the initial case, which shows that the fabricated GaN/AlGaN/GaN SBD has a great potential application in harsh radiation environment of space. The negative polarization charges at the GaN/AlGaN interface effectively free from the effects of traps induced in the radiation process, and make the fabricated devices possess the impressive dynamic characteristics.

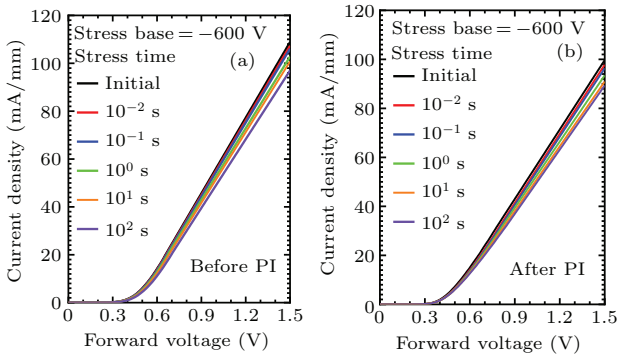



**Fig. 7.** Linear-scale forward *I*–*V* characteristics of fabricated GaN SBDs (a) before and (b) after being irradiated by protons with stress current of 50 mA.

## 4. Conclusions

The proton-irradiation response of the high-performance AlGaN/GaN SBDs passivated with *in-situ* single-crystal GaN layer is demonstrated. The fabricated lateral GaN SBDs irradiated by 10-MeV protons at a fluence of $10^{14}$ cm$^{-2}$ show a more idealized M/S interface and a slighter degradation in forward current than the initial devices. Furthermore, no significant degradation in dynamic characteristics is observed for the irradiated SBDs. The normalized $R_{ON,dyn}$ is found to be only 1.62 times that in the initial case, indicated by a pulse measurement at a quiescent base of −100 V and 14% degradation after experiencing a reverse voltage stress of −600 V for 10 s. These results show that the lateral AlGaN/GaN SBDs passivated with GaN layer have great potential application in space.

## Acknowledgements

Project supported by the National Natural Science Foundation of China (Grant No. 62104185), the Fundamental Research Funds for the Central Universities, China (Grant No. JB211103), the National Natural Science Foundation for Distinguished Young Scholars, China (Grant No. 61925404), and the Wuhu and Xidian University Special Fund for Industry–University-Research Cooperation, China (Grant No. XWYCXY-012021010).

## References

[1] Lei J C, Wei J, G. Tang G F, Zhang Z F, Qian Q K, Zheng Z Y, Hua M Y and Chen K J 2018 *IEEE Electron Dev. Lett.* **39** 260

[2] Zhang T, Zhang Y N, Zhang J C, Li X D, Lv Y G and Hao Y 2021 *IEEE Electron Dev. Lett.* **42** 304

[3] Zhang T, Zhang J, Zhou H, Chen T S, Zhang K, Hu Z Z, Bian Z K, Dang K, Wang Y, Zhang L, Ning J, Ma P J and Hao Y 2018 *IEEE Electron Dev. Lett.* **39** 1548

[4] Xiao M, Ma Y W, Cheng K, Liu K, Xie A, Cao Y and Zhang Y H 2020 *IEEE Electron Dev. Lett.* **41** 1177

[5] Lee H S, Jung D Y, Park Y, Na J, Jang H G, Lee H S, Jun C H, Park J, Ryu S O, Ko S C and Nam E S 2015 *IEEE Electron Dev. Lett.* **36** 1132

[6] Khanna S K, Webb J, Tang H, Houdayer A J and Carlone C 2000 *IEEE Trans Nucl. Sci.* **47** 2322

[7] Hu X, Karmarkar A P, Jun B, Fleetwood D M, Schrimpf R D, Geil R D, Weller R A, White B D, Bataiev M, Brillson L J and Mishra U K 2003 *IEEE Trans Nucl. Sci.* **50** 1791

[8] Anderson T J, Koehler A D, Greenlee J D, Weaver B D, Mastro M A, Hite J K, Eddy C R, Kub F J and Hobart K D 2014 *IEEE Electron Dev. Lett.* **35** 826

[9] Karmarkar A P, Jun B, Fleetwood D M, Schrimpf R D, Weller R A, White B D, Brillson L J and Mishra U K 2004 *IEEE Trans. Nucl. Sci.* **51** 3801

[10] Schwarz C, Yadav A, Shatkhin M, Flitsiyan E, Chernyak L, Kasiyan V, Liu L, Xi Y Y, Ren F, Pearton S J, Lo C F, Johnson J W and Danilova E 2013 *Appl. Phys. Lett.* **102** 062102

[11] Nela L, Yildirim H K, Erine C, Erp R V, Xiang P, Cheng K and Matioli E 2021 *IEEE Electron Dev. Lett.* **42** 86

[12] Nela L, Erp R V, Kampitsis G, Yildirim H K, Ma J and Matioli E 2021 *IEEE Trans. Power Electron.* **36** 1269

[13] Gao J N, J in Y F, Xie B, Wen C P, Hao Y L, Shen B and Wang M J 2018 *IEEE Electron Dev. Lett.* **39** 859

[14] Zhu M D, Song B, Qi M, Hu Z Y, Nomoto K, Yan X D, Cao Y, Johnson W, Kohn E, Jena D and Xing H L 2015 *IEEE Electron Dev. Lett.* **36** 375

[15] Tsou C W, Wei K P, Lian Y W and Hsu S S H 2016 *IEEE Electron Dev. Lett.* **37** 70

[16] Bahat-Treidel E, Hilt O, Zhytnyska R, Wentzel A, Meliani C, Wurfl J and Trankle G 2012 *IEEE Electron Dev. Lett.* **33** 357

[17] Hao R H, Li W Y, Fu K, Yu G H, Song L, Yuan J, Li J S, Deng X G, Zhang X D, Zhou Q, Fan Y M, Shi W H, Cai Y, Zhang X P and Zhang B S 2017 *IEEE Electron Dev. Lett.* **38** 1567

[18] Arulkumaran S, Egawa T and Ishikawa H 2005 *Jpn. J. Appl. Phys.* **44** 2953

[19] Zhang T, Lv Y G, Li R H, Zhang Y N, Zhang Y C, Li X D, Zhang J C and Hao Y 2021 *IEEE Electron Dev. Lett.* **42** 477

[20] Hu J, Stoffels S, Lenci S, Lenci S, Groeseneken G and Decoutere S 2016 *IEEE Electron Dev. Lett.* **37** 310

[21] Hu J, Stoffels S, Lenci S, Ronchi N, Venegas R, You S, Bakeroot B, Groeseneken G and Decoutere S 2014 *Microelectronics Reliability* **54** 2196

[22] Vetury R, Zhang N Q Q, Keller S and Mishra U K 2001 *IEEE Trans. Electron Dev.* **48** 560

[23] Braga N and Mickevicius R 2004 *Appl. Phys. Lett.* **85** 4780

[24] Weaver B D, Martin P A, Boos J B and Cress C D 2012 *IEEE Trans. Nucl. Sci.* **59** 3077

[25] Umana-Membreno G A, Dell J M, Parish G, Nener B D, Faraone L and Mishra U K 2003 *IEEE Trans. Electron Dev.* **50** 2326